Check for updates
Natural Product Sciences
31(1) : 62-73 (2025)
https://doi.org/10.20307/nps.2025.31.1.62

PTP1B Inhibitory Activity of Flavonoids from the Roots of *Astragalus membranaceus* Bunge

Thi Ly Pham[1,2], Manh Tuan Ha[3], Byung Sun Min[3,*], and Jeong Ah Kim[1,2,*]

[1]*Vessel-Organ Interaction Research Center, VOICE (MRC), College of Pharmacy, Kyungpook National University, Daegu 41566, Republic of Korea*
[2]*BK21 FOUR Community-Based Intelligent Novel Drug Discovery Education Unit, College of Pharmacy and Research Institute of Pharmaceutical Sciences, Kyungpook National University, Daegu 41566, Republic of Korea*
[3]*College of Pharmacy, Drug Research and Development Center, Daegu Catholic University, Gyeongbuk 38430, Republic of Korea*

Abstract – The roots of *Astragalus membranaceus* Bunge have long been used in herbal medicine for their diverse biological activities. Notably, its potential anti-diabetic properties have been extensively studied, highlighting promising therapeutic prospects. In this study, we conducted a comprehensive investigation focusing on flavonoid components from the roots of *A. membranaceus* and their PTP1B inhibitory activity. As a result, we isolated a total of 24 flavonoids, among which formonentin (**1**), pratensein (**3**), and vesticarpan (**19**) emerged as the most potent inhibitors against PTP1B with IC_{50} value of 10.9 ± 1.09 μM, 10.0 ± 1.71 μM, and 10.3 ± 1.31 μM, respectively. Additionally, through the enzyme kinetic analysis, the inhibition mode of compound **19** was determined as a competitive inhibitor, with K_i value of 7.6 ± 1.17 μM. Furthermore, the molecular docking simulation elucidated the binding mechanism of compound **19** with PTP1B, mainly through van der Waals forces and hydrogen bonds. This study highlights the PTP1B inhibitory potential of the flavonoid constituents derived from the roots of *A. membranaceus.* Moreover, discovering vesticarpan (**19**) as a novel PTP1B inhibitor provides a significant foundation for further investigations to develop innovative therapeutic strategies for diabetes treatment.
Keywords – *Astragalus membranaceus*, Fabaceae, Flavonoid, PTP1B, Diabetes

Introduction

Diabetes mellitus (DM) is a chronic, non-contagious condition with elevated morbidity levels and costly treatment demands.[1] It is classified into two primary forms: type 1 diabetes (T1D), characterized by deficient insulin production, and type 2 diabetes (T2D), where insulin-responsive cells exhibit resistance. Both types of diabetes demand prolonged treatment, often leading to unforeseen complications and adverse effects on the body.[2] Furthermore, diabetes is recognized as a prevalent risk factor for other chronic conditions, including vision impairments, cardiovascular issues, and neuropathy.[3–5] Therefore, diabetes is considered as a high-risk disease, emphasizing the importance of ongoing research to develop novel therapies. Insulin injection remains the principal treatment for T1D, while T2D is treated using various therapeutic methods targeting specific proteins in the insulin pathway.[6]

Protein-tyrosine phosphatase 1B (PTP1B) has gained attention as a potential therapeutic target for T2D treatment. To date, it has been identified as a therapeutic target for a range of diseases, including diabetes, obesity, cardiovascular disorders, and hematopoietic cancers.[7–10] Until now, although several PTP1B inhibitors have been explored as potential anti-diabetic treatments targeting PTP1B, these agents have faced considerable challenges due to side effects.[11] Hence, it is essential to discover new therapeutic agents from natural resources to minimize the adverse effects associated with long-term treatment.

Flavonoids are the most abundant natural products, attracting significant interest from researchers due to their promising health benefits and nutritional value. Hence, incorporating flavonoid-rich foods into the daily diet is essential to promoting health conditions and eliminating

*Author for correspondence
Byung Sun Min, Ph. D., College of Pharmacy, Daegu Catholic University, Gyeongbuk 38430, Republic of Korea
Tel: +82-53-850-3613; E-mail: bsmin@cu.ac.kr
Jeong Ah Kim, Ph. D., College of Pharmacy, Kyungpook National University, Daegu 41566, Republic of Korea
Tel: +82-53-950-8574; E-mail: jkim6923@knu.ac.kr

the risk of ailments.[12] Among their numerous biological effects, flavonoids have been extensively studied for their anti-diabetic properties. They contribute to diabetes management by regulating carbohydrate digestion, enhancing insulin signaling and secretion, and promoting glucose uptake.[13] Thus, exploring flavonoids as a potential therapeutic strategy for diabetes treatment is crucial.

Astragalus membranaceus Bunge (Fabaceae) has been known for its diverse biological properties, such as immunomodulation, antioxidant properties, antitumor effects, anti-diabetic activity, antiviral actions, hepatoprotection, anti-inflammatory effects, anti-atherosclerotic benefits, hematopoiesis, and neuroprotection.[14] Until now, many studies have been undertaken to evaluate the anti-diabetic effects of phytoconstituents, particularly focusing on several target proteins, including α-amylase, α-glucosidase, and PTP1B.[15–17] Among bioactive secondary metabolisms, astragalus polysaccharides, a key bioactive component derived from the roots of *A. membranaceus*, have emerged as a promising candidate for reducing PTP1B expression.[18] In addition, astragaloside IV, a well-known bioactive component of this plant, was investigated for its anti-diabetic effects through the PTP1B inhibitory mechanism.[19] While polysaccharides demonstrated effectiveness against PTP1B, the potential biological effects of flavonoid components remain unexplored. Although the flavonoid fraction from the roots of *A. membranaceus* showed significant anti-diabetic activity,[20,21] the number of studies focusing on the PTP1B inhibitory effects of flavonoids from the roots of *A. membranaceus* remains limited, leading to gaps in understanding the role of flavonoids from this plant in diabetes treatment, highlighting the need for further investigations.

Therefore, this study aimed to extract the flavonoids from the roots of *A. membranaceus,* investigate their PTP1B inhibitory activity, identify the structure-activity relationships responsible for PTP1B inhibition, and simultaneously elucidate the action mechanism of the most potent inhibitors against PTP1B. As a result, we successfully isolated 24 flavonoids from this plant, categorized into isoflavones (**1**–**10**), isoflavanes (**11**–**16**), flavanone (**17**), chalcone (**18**), and pterocarpans (**19**–**24**). The structures of the isolated compounds were determined using NMR spectroscopy. Additionally, an *in vitro* assay was performed to evaluate the PTP1B inhibitory activity and identify the inhibition mode of the most potent inhibitors. Molecular docking was employed to study the interactions between the most promising ligands and PTP1B.

Experimental

General experimental procedures – Column chromatography (CC) was utilized for the separation process, employing silica gel 60 S (0.060–0.200 mm), silica gel 60 (0.040–0.063 mm), LiChroprep RP-18 (40–63 μm), and MCI gel CHP20P (75–100 μm), provided by Merck (Darmstadt, Germany). Chromatographic separation via HPLC was executed on a Waters Alliance system (Massachusetts, USA) equipped with a 1525 binary pump, a 2998 PDA detector, and a YMC Pack ODS column (20 × 250 mm, 5 μm). Precoated TLC plates with silica gel 60 F_{254} and RP-18 F_{254s} were obtained from Merck (Darmstadt, Germany). The spots were examined for UV absorbance at 254 and 365 nm, treated with 10% sulfuric acid spray, and heated at 100°C for 1 minute. NMR spectra acquisition was carried out with a Bruker Avance 500 MHz spectrometer (Bruker, Karlsruhe, Germany). Optical rotations were acquired using a JASCO P2000 polarimeter (JASCO, Tokyo, Japan). All solvents required for these experiments were obtained from Fisher Scientific Korea Ltd. (Seoul, Korea).

Plant materials – The roots of *Astragalus membranaceus* Bunge were obtained from a traditional market in Jeonju, Korea, in March of 2023 and authenticated by Professor Byung Sun Min at Daegu Catholic University. A documented specimen (26A-AMR) was archived at the Pharmacognosy Laboratory in the College of Pharmacy, Kyungpook National University, Korea.

Extraction and isolation – The dried roots (14.8 kg) of *A. membranaceus* were extracted three times using methanol (MeOH, 15 L for 4 hours each). The MeOH extract (2.1 kg) was dissolved in H_2O and then partitioned sequentially with *n*-hexane, methylene chloride (CH_2Cl_2), ethyl acetate (EtOAc), and *n*-butanol (BuOH). The CH_2Cl_2 and EtOAc layers (67.6 g) were combined and subfractioned through vacuum liquid chromatography (VLC) (CH_2Cl_2: MeOH: H_2O; 20:1:0 → 2:1:0.2, v/v/v) to obtain 4 subfractions (1A–1D). The fraction 1A was separated into 4 subfractions (2A–2D) using CC, silica gel (CH_2Cl_2:MeOH:H_2O; 20:1:0 → 2:1:0.2, v/v/v). From fraction 2B, 9 subfractions (3A–3I) were obtained using silica gel column chromatography (CC) RP-18 (MeOH:H_2O; 1:2 → 1:0, v/v). The fraction 3H was then loaded on CC, silica gel (CH_2Cl_2:acetone; 20:1 → 0:1, v/v) to obtain compound **1**. The fractions 3D and 3E were combined and analyzed in CC, silica gel (CH_2Cl_2:acetone; 25:1 → 0:1, v/v) to obtain compound **20**. The fraction 3G was then purified through CC, silica gel (CH_2Cl_2:acetone; 20:1

→ 0:1, v/v) to gain compound **4**, while fraction 3F was applied on CC, silica gel (Hexane:EtOAc; 2:1 → 0:1, v/v) to obtain compounds **11** and **16**. Fraction 2C was separated into 12 subfractions (4A–4L) by using CC, silica gel (CH_2Cl_2:EtOAc; 20:1 → 0:1, v/v). Compound **2** was isolated from subfraction 4L by silica gel CC (CH_2Cl_2:acetone; 10:1, v/v), and compound **17** was purified from subfraction 4J through CC, RP-18 (MeOH:H_2O; 1:2 → 1:0, v/v), while compounds **3**, **5** and **18** were isolated from subfraction 4G in the same isolating condition. The mixture of fractions 4C and 4D was separated into 11 subfractions (5A–5J) through CC, RP-18 (acetone:H_2O; 1:2 → 1:0, v/v). Subfaction 5G was determined as compound **15**, while compounds **19** and **21** were isolated from subfraction 5E. Fraction 1B was fractionated into 6 subfractions (6A–6E) by using MCI gel (MeOH:H2O; 1:2 → 1:0, v/v). Compounds **23** was crystalized in MeOH from fraction 6B. From fraction 6D, 6 subfractions (8A–8F) were obtained through eluting on CC, RP-18 (MeOH:H_2O; 3:2, v/v). From fraction 8D, compound **24** was isolated using silica gel CC (CH_2Cl_2:MeOH:H_2O; 20:1:0 → 10:1:0.1, v/v/v). Fraction 8C was divided into 3 subfractions (9A–9C) by eluting on RP-18 CC (acetone:H_2O; 6:5 → 1:0, v/v). Fraction 9B was then separated into 7 subfractions (10A–10G) through silica gel CC (CH_2Cl_2:MeOH:H_2O; 25:1:0 → 8:1:0.05, v/v/v). Compounds **7** and **13** were isolated from fraction 10F by using silica gel CC (CH_2Cl_2:EtOAc; 1:10 → 1:20, v/v). Fraction 6C was continuously separated into 10 subfractions (11A–11J) by eluting on RP-18 CC (MeOH:H_2O; 1:2 → 1:0, v/v), in which fraction 11G was determined as compound **10**. Fractions 1C and 1D were combined and analyzed on silica gel CC (CH_2Cl_2:MeOH; 2:1 → 0:1, v/v) to obtain 6 subfractions (12A–12F). From the mixture of fraction 12B and 12C, compound **12** was crystalized in MeOH, and the remaining part was loaded on RP-18 CC (acetone:H_2O; 1:3 → 1:0, v/v) to separate into 8 subfractions (13A–13H). From fraction 13B, compounds **9** and **22** were isolated through RP-18 CC (MeOH:H_2O; 1:3 → 1:0, v/v). Fraction 12D was loaded on silica gel CC (CH_2Cl_2:MeOH; 15:1, v/v) to separate into 3 subfractions (15A–15C). Fraction 15C was fractionated into 4 subfractions (16A–16D) through RP-18 CC (MeOH:H_2O; 1:2 → 1:0, v/v). Compound **8** was obtained from fraction 16B by eluting on RP-18 CC (MeOH:H_2O; 2:5, v/v).

The *n*-BuOH layer (139.7 g) was separated into 6 fractions (18A–18F) through silica gel CC (CH_2Cl_2:MeOH; 1:0 → 1:1, v/v). From fraction 18C, 6 subfractions (19A–19F) were obtained by eluting on RP-18 CC (MeOH:H_2O; 2:3 → 1:0, v/v), then fraction 19D was loaded on silica gel CC (CH_2Cl_2:MeOH; 10:1, v/v) to purify compound **6**. Fraction 18F was loaded on silica gel CC (EtOAc:MeOH:H_2O; 3:1:0 → 2:1:0.2, v/v/v) to separate into 3 fractions (25A–25C). From fraction 25B, 9 subfractions (26A–26I) were obtained by using MCI gel CC (acetone:H_2O; 1:3 → 1.1, v/v). Compound **14** were isolated from fraction 26B through RP-18 CC (MeOH:H_2O 1:2 → 1:1, v/v).

Formonentin (1) – White amorphous powder; ^{1}H-NMR (500 MHz, DMSO-d_6): δ 8.33 (1H, s, H-2), 8.00 (1H, d, J = 8.76 Hz, H-5), 6.93 (1H, dd, J = 2.2, 8.77 Hz, H-6), 6.87 (1H, d, J = 2.20 Hz, H-8), 7.50 (1H, d, J = 8.78 Hz, H-2′), 6.98, (1H, d, J = 8.81 Hz, H-3′), 6.98, (1H, d, J = 8.81 Hz, H-5′), 7.50 (1H, d, J = 8.78 Hz, H-6′), 3.78 (3H, s, OCH_3); ^{13}C-NMR (125 MHz, DMSO-d_6): δ 153.1 (C-2), 123.1 (C-3), 174.6 (C-4), 116.6 (C-4a), 127.3 (C-5), 115.2 (C-6), 162.6 (C-7), 102.1 (C-8), 157.4 (C-8a), 124.2 (C-1′), 130.1 (C-2′ and C-6′), 113.6 (C-3′and C-5′), 158.9 (C-4′), 55.1 (OCH_3).

Calycosin (2) – White amorphous powder; ^{1}H-NMR (500 MHz, CD_3OD): δ 8.12 (1H, s, H-2), 8.06 (1H, d, J = 8.83 Hz, H-5), 6.94 (1H, dd, J = 2.28, 8.83 Hz, H-6), 6.85 (1H, d, J = 2.25 Hz, H-8), 7.05 (1H, s, H-2′), 6.97 (2H, br s, H-5′ and H-6′), 3.89 (3H, s, OCH_3); ^{13}C-NMR (125 MHz, CD_3OD): δ 154.8 (C-2), 125.7 (C-3), 178.0 (C-4), 118.2 (C-4a), 128.5 (C-5), 116.5 (C-6), 164.7 (C-7), 103.2 (C-8), 159.7 (C-8a), 126.2 (C-1′), 117.4 (C-2′), 147.4 (C-3′), 149.1 (C-4′), 112.6 (C-5′), 121.6 (C-6′), 56.4 (OCH_3).

Pratensein (3) – Pale yellow amorphous powder; ^{1}H-NMR (500 MHz, DMSO-d_6): δ 8.31 (1H, s, H-2), 6.21 (1H, d, J = 2.06 Hz, H-6), 6.37 (1H, d, J = 2.04 Hz, H-8), 7.03 (1H, d, J = 1.99 Hz, H-2′), 6.97 (1H, d, J = 8.38 Hz, H-5′), 6.93 (1H, dd, J = 2.01, 8.29 Hz, H-6′), 3.79 (3H, s, OCH_3); ^{13}C-NMR (125 MHz, DMSO-d_6): δ 154.1 (C-2), 123.3 (C-3), 180.0 (C-4), 104.3 (C-4a), 161.9 (C-5), 99.0 (C-6), 164.7 (C-7), 93.7 (C-8), 157.5 (C-8a), 122.1 (C-1′), 116.3 (C-2′), 146.1 (C-3′), 147.7 (C-4′), 112.0 (C-5′), 119.7 (C-6′), 55.6 (OCH_3).

Afromorsin (4) – Yellow amorphous powder; ^{1}H-NMR (500 MHz, DMSO-d_6): δ 8.29 (1H, s, H-2), 7.39 (1H, s, H-5), 6.95 (1H, s, H-8), 7.52 (2H, d, J = 8.81 Hz, H-2′ and H-6′), 6.98 (2H, d, J = 8.84 Hz, H-3′ and H-5′), 3.86 (3H, s, 6-OCH_3), 3.78 (3H, s, 4′-OCH_3); ^{13}C-NMR (125 MHz, DMSO-d_6): δ 152.4 (C-2), 122.3 (C-3), 174.1 (C-4), 115.1 (C-4a), 104.2 (C-5), 147.3 (C-6), 152.5 (C-7), 102.5 (C-8), 152.0 (C-8a), 124.5 (C-1′), 129.9 (C-2 and C-6′), 113.4 (C-3′ and C-5′), 158.7 (C-4′), 55.7 (6-OCH_3), 55.1 (4′-OCH_3).

Odoratin (5) – White amorphous powder; ^{1}H-NMR (500 MHz, CD_3OD): δ 8.15 (1H, s, H-2), 7.57 (1H, s, H-5), 6.93 (1H, s, H-8), 7.07 (1H, s, H-2′), 6.99 (2H, overlapped, H-5′ and H-6′), 3.96 (3H, s, 6-OCH_3), 3.98 (3H, s, 4′-

OCH_3); ^{13}C-NMR (125 MHz, CD_3OD): δ 154.6 (C-2), 125.3 (C-3), 177.7 (C-4), 117.8 (C-4a), 105.4 (C-5), 148.8 (C-6), 154.6 (C-7), 103.7 (C-8), 154.5 (C-8a), 126.4 (C-1′), 117.5 (C-2′), 147.4 (C-3′), 149.1 (C-4′), 112.7 (C-5′), 121.6 (C-6′), 56.6 (6-OCH_3), 56.4 (4′-OCH_3).

Ononin (6) – White amorphous powder; ^{1}H-NMR (500 MHz, DMSO-d_6): δ 8.43 (1H, s, H-2), 8.06 (1H, d, J = 8.87 Hz, H-5), 7.15 (1H, dd, J = 2.24, 8.88 Hz, H-6), 7.24 (1H, d, J = 2.20 Hz, H-8), 7.53 (2H, d, J = 8.73 Hz, H-2′ and H-6′), 7.00 (2H, d, J = 8.77 Hz, H-3′ and H-5′), 5.11 (1H, d, J = 7.22 Hz, H-1″), 3.31 (1H, m, H-2″), 3.47 (2H, overlapped, H-3″ and H-6″α), 3.18 (1H, m, H-4″), 3.32 (1H, m, H-5″), 3.73 (1H, m, H-6″β), 3.79 (3H, s, 4′-OCH_3); ^{13}C-NMR (125 MHz, DMSO-d_6): δ 153.6 (C-2), 124.0 (C-3), 174.7 (C-4), 118.5 (C-4a), 127.0 (C-5), 115.6 (C-6), 161.5 (C-7), 103.4 (C-8), 157.1 (C-8a), 123.4 (C-1′), 130.1 (C-2′ and C-6′), 113.6 (C-3′ and C-5′), 159.0 (C-4′), 100.0 (C-1″), 73.1 (C-2″), 77.2 (C-3″), 69.6 (C-4″), 76.5 (C-5″), 60.6 (C-6″), 55.2 (4′-OCH_3).

6″-*O*-Acetylononin (7) – Pale yellow amorphous powder; ^{1}H-NMR (500 MHz, CD_3OD): δ 8.22 (1H, s, H-2), 8.15 (1H, d, J = 8.86 Hz, H-5), 7.20 (1H, dd, J = 2.21, 8.96 Hz, H-6), 7.22 (1H, d, J = 2.10 Hz, H-8), 7.49 (2H, d, J = 8.74 Hz, H-2′ and H-6′), 6.99 (2H, m, H-3′ and H-5′), 5.12 (1H, m, H-1″), 3.55 (2H, overlapped, H-2″ and H-3″), 3.43 (1H, m, H-4″), 3.79 (1H, m, H-5″), 4.48 (1H, m, H-6″α), 4.25 (1H, m, H-6″β), 3.84 (3H, s, $COCH_3$), 2.10 (3H, s, 4′-OCH_3); ^{13}C-NMR (125 MHz, CD_3OD): δ 155.2 (C-2), 126.0 (C-3), 177.9 (C-4), 120.3 (C-4a), 128.3 (C-5), 117.1 (C-6), 163.3 (C-7), 105.0 (C-8), 159.1 (C-8a), 125.3 (C-1′), 131.3 (C-2′ and C-6′), 114.9 (C-3′ and C-5′), 161.2 (C-4′), 101.7 (C-1″), 74.7 (C-2″), 77.7 (C-3″), 71.5 (C-4″), 75.6 (C-5″), 64.7 (C-6″), 172.6 ($\underline{C}OCH_3$), 20.7 ($CO\underline{C}H_3$), 55.7 (4′-OCH_3).

Calycosin 7-*O*-β-D-glucoside (8) – White amorphous powder; ^{1}H-NMR (500 MHz, DMSO-d_6): δ 8.36 (1H, s, H-2), 8.06 (1H, d, J = 8.75 Hz, H-5), 7.15 (1H, dd, J = 2.50, 8.49 Hz, H-6) 7.23 (1H, d, J = 2.5 Hz, H-8), 7.09 (1H, m, H-2′), 6.96 (2H, overlapped, H-5′ and H-6′), 5.12 (1H, br d, H-1″), 3.35 (2H, m, H-2″ and H-3″), 3.22 (1H, m, H-4″), 3.49 (2H, m, H-5″ and H-6″β), 3.77 (1H, m, H-6″α), 3.79 (3H, s, 4′-OCH_3); ^{13}C-NMR (125 MHz, DMSO-d_6): δ 153.6 (C-2), 123.7 (C-3), 174.8 (C-4), 118.6 (C-4a), 127.1 (C-5), 115.7 (C-6), 161.5 (C-7), 103.5 (C-8), 157.1 (C-8a), 124.4 (C-1′), 116.5 (C-2′), 146.1 (C-3′), 147.7 (C-4′), 112.0 (C-5′), 119.8 (C-6′), 100.1 (C-1″), 73.2 (C-2″), 76.6 (C-3″) 69.7 (C-4″), 77.3 (C-5″), 60.8 (C-6″), 55.7 (4′-OCH_3).

Calycosin 7-*O*-β-D-glucoside-6″-*O*-acetate (9) – Yellow amorphous powder; ^{1}H NMR (500 MHz, CD_3OD): δ 8.18 (1H, s, H-2), 8.17 (1H, d, J = 8.85 Hz, H-5), 7.23 (1H, m, H-6), 7.25 (1H, br d, H-8), 7.09 (1H, br s, H-2′), 7.02 (2H, br s, H-5′ and H-6′), 5.13 (1H, m, H-1″), 3.56 (2H, m, H-2″ and H-3″), 3.44 (1H, m, H-4″), 3.80 (1H, m, H-5″), 4.50 (1H, m, H-6″α), 4.27 (1H, m, H-6″β), 3.92 (3H, s, $COCH_3$), 2.11 (3H, s, 4′-OCH_3); ^{13}C-NMR (125 MHz, CD_3OD): δ 155.2 (C-2), 125.9 (C-3), 177.9 (C-4), 120.3 (C-4a), 128.3 (C-5), 117.1 (C-6), 163.3 (C-7), 105.0 (C-8), 159.1 (C-8a), 126.1 (C-1′), 117.4 (C-2′), 147.4 (C-3′), 149.3 (C-4′), 112.7 (C-5′), 121.6 (C-6′), 101.7 (C-1″), 74.7 (C-2″), 77.7 (C-3″), 71.5 (C-4″) 75.6 (C-5″), 64.7 (C-6″), 172.7 ($\underline{C}OCH_3$), 20.7 ($CO\underline{C}H_3$), 56.4 (4′-OCH_3).

Calycosin 7-*O*-β-D-{6″-[(*E*)-but-2-enoyl]}-glucoside (10) – Yellow amorphous powder; ^{1}H-NMR (500 MHz, DMSO-d_6): δ 8.83 (1H, s, H-2), 8.04 (1H, d, J = 8.86 Hz, H-5), 7.13 (1H, dd, J = 1.77, 8.90 Hz, H-6), 7.19 (1H, d, J = 1.74 Hz, H-8), 7.07 (1H, brs, H-2′), 6.96 (2H, br s, H-5′ and H-6′), 5.18 (1H, d, J = 6.97 Hz, H-1″), 3.36 (2H, m, H-2″ and H-5″), 3.80 (1H, m, H-3″), 3.23 (1H, m, H-4″), 4.14 (1H, br d, H-6″α), 4.13 (1H, br d, H-6″β), 5.88 (1H, d, J = 15.49 Hz, H-2‴), 6.88 (1H, dd, J = 6.96, 15.46 Hz, H-3‴), 1.83 (3H, d, J = 6.32 Hz, H-4‴), 3.79 (3H, s, 4′-OCH_3); ^{13}C-NMR (125 MHz, DMSO-d_6): δ 153.6 (C-2), 124.5 (C-3), 174.7 (C-4), 118.6 (C-4a), 127.0 (C-5), 115.6 (C-6), 161.2 (C-7), 103.4 (C-8), 157.0 (C-8a), 123.7 (C-1′), 116.5 (C-2′), 146.1 (C-3′), 147.7 (C-4′), 112.0 (C-5′), 119.8 (C-6′), 99.6 (C-1″), 73.1 (C-2″), 73.9 (C-3″), 70.1 (C-4″), 76.3 (C-5″), 63.3 (C-6″), 165.3 (C-1‴), 122.1 (C-2‴), 145.4 (C-3‴), 17.7 (C-4‴), 55.7 (4′-OCH_3).

Isomucronulatol (11) – White amorphous powder; $[\alpha]_D^{25}$ –11.67 (*c* 0.02, MeOH); ^{1}H-NMR (500 MHz, CD_3OD): δ 4.25 (1H, ddd, J = 2.01, 3.38, 10.29 Hz, H-2α), 3.97 (1H, t, J = 10.1 Hz, H-2β), 3.47 (1H, m, H-3), 2.95 (1H, dd, J = 10.87, 15.48 Hz, H-4α), 2.80 (1H, ddd, J = 1.49, 5.06, 15.62 Hz, H-4β), 6.88 (1H, d, J = 8.23 Hz, H-5), 6.35 (1H, dd, J = 2.47, 8.22 Hz, H-6), 6.27 (1H, d, J = 2.44 Hz, H-8), 6.46 (1H, d, J = 8.67 Hz, H-5′), 6.77 (1H, d, J = 8.65 Hz, H-6′), 3.82 (6H, br s, 3′-OCH_3 and 4′-OCH_3); ^{13}C-NMR (125 MHz, CD_3OD): δ 70.9 (C-2), 33.5 (C-3), 31.2 (C-4), 114.8 (C-4a), 131.2 (C-5), 109.3 (C-6), 157.0 (C-7), 103.8 (C-8), 156.3 (C-8a), 122.4 (C-1′), 149.5 (C-2′), 137.5 (C-3′), 153.1 (C-4′), 104.4 (C-5′), 122.8 (C-6′), 56.2 (3′-OCH_3), 61.0 (4′-OCH_3).

Isomucronulatol 7-*O*-β-glucoside (12) – White, crystalline powder; $[\alpha]_D^{25}$ –43.55 (*c* 0.02, MeOH); ^{1}H-NMR (500 MHz, DMSO-d_6): δ 4.19 (1H, ddd, J = 10.5 Hz, 3.5 Hz, 1.7 Hz, H-2α), 3.96 (1H, t, J = 10.02 Hz, H-2β), 3.36 (1H, m, H-3), 2.93 (1H, dd, J=10.6, 15.85 Hz, H-4α), 2.80 (1H, dd, J = 4.3, 15.82 Hz, H-4β), 7.00 (1H, d, J = 8.43 Hz, H-5), 6.55 (1H, dd, J = 2.36, 8.33 Hz, H-6), 6.47 (1H,

d, J = 2.46 Hz, H-8), 6.46 (1H, d, J = 8.55 Hz, H-5′), 6.78 (1H, d, J = 8.66 Hz, H-6′), 4.77 (1H, d, J = 7.63 Hz, H-1″), 3.20 (1H, m, H-2″), 3.28 (2H, m, H-3″ and H-5″), 3.14 (1H, m, H-4″), 3.69 (1H, overlapped, H-6″α), 3.46 (1H, m, H-6″β), 3.68 (3H, s, 3′-OCH_3), 3.74 (3H, s, 4′-OCH_3); ^{13}C-NMR (125 MHz, DMSO-d_6): δ 69.2 (C-2), 31.3 (C-3), 29.7 (C-4), 115.8 (C-4a), 130.0 (C-5), 108.8 (C-6), 156.7 (C-7), 103.8 (C-8), 154.5 (C-8a), 120.8 (C-1′), 148.1 (C-2′), 136.2 (C-3′), 151.7 (C-4′), 103.2 (C-5′), 121.4 (C-6′), 100.7 (C-1″), 73.2 (C-2″), 76.6 (C-3″), 69.8 (C-4″), 77.0 (C-5″), 60.7 (C-6″), 60.2 (3′-OCH_3), 55.6 (4′-OCH_3).

2′-Hydroxy-3′,4′-dimethoxyisoflavan 7-*O*-β-D-glucoside 6″-*O*-acetate (13) – White amorphous powder; $[\alpha]_D^{25}$ –36.48 (c 0.04, MeOH); ^{1}H-NMR (500 MHz, CD_3OD): δ 4.29 (1H, m, H-2α), 4.03 (1H, t, J = 10.04 Hz, H-2β), 3.48 (1H, overlapped, H-3), 3.02 (1H, dd, J = 10.59, 15.84 Hz, H-4α), 2.88 (1H, m, H-4β), 7.00 (1H, d, J = 8.35 Hz, H-5), 6.61 (1H, dd, J = 2.48, 8.34 Hz, H-6), 6.57 (1H, d, J = 2.45 Hz, H-8), 6.48 (1H, d, J = 8.70 Hz, H-5′), 6.80 (1H, d, J = 8.66 Hz, H-6′), 4.84 (1H, d, J = 7.46 Hz, H-1″), 3.47 (1H, m, H-2″), 3.65 (1H, m, H-3″), 3.38 (1H, m, H-4″), 3.48 (1H, m, H-5″), 4.42 (1H, dd, J = 2.20, 11.81 Hz, H-6″α), 4.19 (1H, m, H-6″β), 2.08 (3H, s, $COCH_3$), 3.82 (3H, s, 3′-OCH_3), 3.83 (3H, s, 4′-OCH_3); ^{13}C-NMR (125 MHz, CD_3OD): δ 71.0 (C-2), 33.4 (C-3), 31.3 (C-4), 117.9 (C-4a), 131.1 (C-5), 110.4 (C-6), 158.2 (C-7), 105.6 (C-8), 156.3 (C-8a), 122.3 (C-1′), 149.5 (C-2′), 137.6 (C-3′), 153.2 (C-4′), 104.4 (C-5′), 122.8 (C-6′), 102.4 (C-1″), 74.9 (C-2″), 75.3 (C-3″), 71.8 (C-4″), 77.9 (C-5″), 64.8 (C-6″), 172.8 ($\underline{C}OCH_3$), 20.7 ($CO\underline{C}H_3$), 61.1 (3′-OCH_3), 56.3 (4′-OCH_3).

Isomucronulatol 2′,7-diglucoside (14) – White amorphous powder; $[\alpha]_D^{25}$ –21.78 (c 0.04, MeOH); ^{1}H-NMR (500 MHz, CD_3OD): δ 4.4 (1H, m, H-2α), 3.91 (1H, m, H-2β), 3.82 (1H, m, H-3), 2.91 (1H, dd, J = 11.05, 15.86 Hz, H-4α), 2.82 (1H, dd, J = 4.66, 15.45 Hz, H-4β), 6.99 (1H, d, J = 8.39 Hz, H-5), 6.65 (1H, dd, J = 2.4, 8.36 Hz, H-6), 6.60 (1H, d, J = 2.44 Hz, H-8), 6.83 (1H, d, J = 8.78 Hz, H-5′), 6.91 (1H, d, J = 8.74 Hz, H-6′), 4.89 (1H, m, H-1″), 3.46 (2H, m, H-2″ and H-3″), 3.44 (2H, m, H-4″ and H-3‴), 3.45 (1H, m, H-5″), 3.93 (1H, m, H-6″α), 3.70 (1H, m, H-6″β), 5.06 (1H, m, H-1‴), 3.47 (1H, m, H-2‴), 3.38 (1H, m, H-4‴), 3.35 (1H, m, H-5‴), 3.92 (1H, m, H-6‴α), 3.72 (1H, m, H-6‴β), 3.87 (3H, s, 3′-OCH_3), 3.86 (3H, s, 4′-OCH_3); ^{13}C-NMR (125 MHz, CD_3OD): δ 71.7 (C-2), 32.1 (C-3), 32.5 (C-4), 118.0 (C-4a). 131.2 (C-5), 110.3 (C-6), 158.4 (C-7), 105.7 (C-8), 156.3 (C-8a), 130.2 (C-1′), 149.2 (C-2′), 143.0 (C-3′), 153.9 (C-4′), 109.9 (C-5′), 122.9 (C-6′), 102.5 (C-1″), 75.1 (C-2″), 77.9 (C-3″), 71.3 (C-4″), 78.1 (C-5″), 62.8 (C-6″), 105.1 (C-1‴), 74.9 (C-2‴), 77.8 (C-3‴), 71.6 (C-4‴), 78.3 (C-5‴), 62.4 (C-6‴), 61.6 (3′-OCH_3), 56.5 (4′-OCH_3).

Pendulone (15) – Reddish crystalline powder; $[\alpha]_D^{25}$ –19.05 (c 0.02, MeOH); ^{1}H NMR (500 MHz, CD_3OD): δ 4.24 (1H, ddd, J = 1.3, 3.04, 10.64, H-2α), 3.98 (1H, m, H-2β), 3.37 (1H, d, J = 7.23 Hz, H-3), 2.95 (1H, dd, J = 5.61, 15.8 Hz, H-4α), 2.74 (1H, dd, J = 7.93, 15.84 Hz, H-4β), 6.89 (1H, d, J = 8.32 Hz, H-5), 6.36 (1H, dd, J = 2.46, 8.26 Hz, H-6), 6.25 (1H, d, J = 2.44 Hz, H-8), 6.40 (1H, s, H-6′), 4.01 (6H, br s, 3′-OCH_3 and 4′-OCH_3); ^{13}C-NMR (125 MHz, CD_3OD): δ 69.4 (C-2), 32.4 (C-3), 30.7 (C-4), 112.8 (C-4a), 131.2 (C-5), 109.7 (C-6), 158.0 (C-7), 103.9 (C-8), 156.0 (C-8a), 148.2 (C-1′), 184.8 (C-2′), 146.7 (C-3′), 146.1 (C-4′), 184.4 (C-5′), 131.9 (C-6′), 61.7 (3′-OCH_3), 61.6 (4′-OCH_3).

4,7,2′-Trihydroxy-4′-methoxyisoflavanol (16) – Yellow powder; $[\alpha]_D^{25}$ –170.01 (c 0.02, MeOH); ^{1}H-NMR (500 MHz, CD_3OD) δ 4.24 (1H, dd, J = 2.83, 8.59 Hz, H-2α), 3.54 (1H, m, H-2β), 4.56 (1H, m, H-3), 5.49 (1H, d, J = 6.36 Hz, H-4), 7.31 (1H, d, J = 8.43 Hz, H-5), 6.52 (1H, dd, J = 2.43, 8.40 Hz, H-6), 6.33 (1H, d, J = 2.41 Hz, H-8), 6.41 (1H, d, J = 2.26 Hz, H-3′), 6.46 (1H, dd, J = 2.28, 8.18 Hz, H-5′), 7.19 (1H, d, J = 8.19 Hz, H-6′); ^{13}C-NMR (125 MHz, CD_3OD): δ 67.5 (C-2), 40.9 (C-3), 80.1 (C-4), 112.9 (C-4a), 133.1 (C-5), 110.7 (C-6), 160.1 (C-7), 104.9 (C-8), 158.1 (C-8a), 120.8 (C-1′), 162.1 (C-2′), 97.6 (C-3′), 162.6 (C-4′), 107.2 (C-5′), 125.9 (C-6′).

(2*S*)-Liquiritigenin (17) – Pale yellow powder; $[\alpha]_D^{25}$ –18.30 (c 0.08, MeOH); ^{1}H-NMR (500 MHz, CD_3OD) δ 5.41 (1H, dd, J = 2.88, 13.6 Hz, H-2), 3.08 (1H, dd, J = 13.07, 16.91 Hz, H-3α), 2.72 (1H, dd, J = 2.96, 16.91 Hz, H-3β), 7.76 (1H, d, J = 8.76 Hz, H-5), 6.55 (1H, dd, J = 2.27, 8.72 Hz, H-6), 6.38 (1H, d, J = 2.24 Hz, H-8), 7.35 (1H, d, J = 8.47 Hz, H-2′), 6.84 (1H, d, J = 8.63 Hz, H-3′), 6.83 (1H, d, J = 8.63 Hz, H-5′), 7.35 (1H, d, J = 8.47 Hz, H-6′); ^{13}C-NMR (125 MHz, CD_3OD): δ 81.1 (C-2), 44.6 (C-3), 193.5 (C-4), 115.0 (C-4a), 129.9 (C-5), 111.7 (C-6), 166.8 (C-7), 103.8 (C-8), 165.6 (C-8a), 131.4 (C-1′), 129.0 (C-2′), 116.3 (C-3′), 158.9 (C-4′), 116.3 (C-5′), 129.0 (C-6′).

Isoliquiritigenin (18) – Yellow crystalline powder; ^{1}H-NMR (500 MHz, CD_3OD) δ 7.64 (2H, d, J = 8.91 Hz, H-2 and H-6), 6.86 (2H, d, J = 8.60 Hz, H-3 and H-5), 6.31 (1H, d, J = 2.37 Hz, H-3′), 6.43 (1H, dd, J = 2.37, 8.87 Hz, H-5′), 7.99 (1H, d, J = 8.91 Hz, H-6′), 7.64 (1H, overlapped, CH-α), 7.80 (1H, d, J = 15.35 Hz, CH-β); ^{13}C-NMR (125 MHz, CD_3OD): δ 127.9 (C-1), 131.8 (C-2 and C-6), 116.9 (C-3 and C-5), 161.6 (C-4), 114.7 (C-1′), 166.5 (C-2′), 103.9 (C-3′), 167.5 (C-4′), 109.2 (C-5′),

133.4 (C-6′), 118.4 (CH-*α*), 145.6 (CH-*β*), 193.5 (C=O).

Vesticarpan (19) – Pale yellow powder; $[\alpha]_D^{25}$ –155.69 (*c* 0.02, MeOH); ^{1}H-NMR (500 MHz, CD_3OD) *δ* 7.37 (1H, d, *J* = 8.43 Hz, H-1), 6.52 (1H, dd, *J* = 2.44, 8.40 Hz, H-2), 6.33 (1H, d, *J* = 2.40 Hz, H-4), 4.24 (1H, dd, *J* = 4.33, 10.40 Hz, H-6*α*), 3.57 (1H, t, *J* = 10.40 Hz, H-6*β*), 3.52 (1H, ddd, *J* = 4.33, 6.20, 10.40 Hz, H-6a), 6.77 (1H, d, *J* = 8.19 Hz, H-7), 6.52 (1H, d, *J* = 8.13 Hz, H-8), 5.50 (1H, d, *J* = 6.24 Hz, H-11a), 3.84 (3H, s, 9-OCH_3); ^{13}C-NMR (125 MHz, CD_3OD): *δ* 133.4 (C-1), 110.7 (C-2), 160.1 (C-3), 104.0 (C-4), 158.0 (C-4a), 67.5 (C-6), 41.5 (C-6a), 122.9 (C-6b), 115.6 (C-7), 105.8 (C-8), 150.5 (C-9), 132.5 (C-10), 148.6 (C-10a), 80.4 (C-11a), 112.8 (C-11b), 56.7 (9-OCH_3).

Methylnissolin (20) – White, amorphous powder; $[\alpha]_D^{25}$ –177.97 (*c* 0.04, MeOH); ^{1}H-NMR (500 MHz, CD_3OD) *δ* 6.97 (1H, d, *J* = 8.16 Hz, H-1), 6.52 (1H, m, H-2), 6.33 (1H, d, *J* = 2.40 Hz, H-4), 4.24 (1H, dd, *J* = 4.01, 10.30 Hz, H-6*α*), 3.60 (1H, t, *J* = 10.30 Hz, H-6*β*), 3.54 (1H, ddd, *J* = 4.01, 6.31, 10.30 Hz, H-6a), 6.97 (1H, d, *J* = 8.16 Hz, H-7), 6.54 (1H, d, *J* = 8.24 Hz, H-8), 5.53 (1H, d, *J* = 6.52 Hz, H-11a), 3.82 (3H, s, 9-OCH_3), 3.85 (3H, s, 10-OCH_3); ^{13}C-NMR (125 MHz, CD_3OD): *δ* 133.3 (C-1), 110.7 (C-2), 160.2 (C-3), 104.1 (C-4), 158.0 (C-4a), 67.3 (C-6), 41.2 (C-6a), 123.5 (C-6b), 119.8 (C-7), 106.2 (C-8), 154.4 (C-9), 135.7 (C-10), 152.6 (C-10a), 80.7 (C-11a), 112.7 (C-11b), 56.8 (9-OCH_3), 60.9 (10-OCH_3).

(6a*R*,11a*R*)-3,8-Dihydroxy-9,10-dimethoxypterocarpan (21) – Yellow powder; $[\alpha]_D^{25}$ –93.49 (*c* 0.02, MeOH); ^{1}H-NMR (500 MHz, CD_3OD) *δ* 7.33 (1H, d, *J* = 8.42 Hz, H-1), 6.51 (1H, dd, *J* = 8.40, 2.42 Hz, H-2), 6.33 (1H, d, *J* = 2.39 Hz, H-4), 4.23 (1H, dd, *J* = 4.95, 10.70 Hz, H-6*α*), 3.62 (1H, t, *J* = 10.70 Hz, H-6*β*), 3.48 (1H, ddd, *J* = 10.70, 6.80, 4.95 Hz, H-6a), 6.58 (1H, s, H-7), 5.45 (1H, d, *J* = 6.85 Hz, H-11a), 3.81 (3H, s, 9-OCH_3), 3.93 (3H, s, 10-OCH_3); ^{13}C-NMR (125 MHz, CD_3OD): *δ* 133.2 (C-1), 110.7 (C-2), 160.1 (C-3), 104.0 (C-4), 158.0 (C-4a), 67.2 (C-6), 41.8 (C-6a), 124.8 (C-6b), 107.1 (C-7), 144.9 (C-8), 141.2 (C-9), 139.5 (C-10), 145.9 (C-10a), 79.8 (C-11a), 112.9 (C-11b), 61.5 (9-OCH_3), 60.8 (10-OCH_3).

Licoagroside D (22) – Yellow amorphous powder; $[\alpha]_D^{25}$ –191.81 (*c* 0.02, MeOH); ^{1}H-NMR (500 MHz, CD_3OD): *δ* 7.45 (1H, d, *J* = 8.63 Hz, H-1), 6.79 (1H, dd, *J* = 2.45, 8.55 Hz, H-2), 6.64 (1H, d, *J* = 2.42 Hz, H-4), 4.24 (1H, dd, *J* = 3.96, 10.20 Hz, H-6*α*), 3.55 (1H, t, *J* = 10.20 Hz, H-6*β*), 3.54 (1H, ddd, *J* = 10.20, 6.20, 3.96 Hz, H-6a), 7.73 (1H, d, *J* = 8.18 Hz, H-7), 6.49 (1H, d, *J* = 8.18 Hz, H-8), 5.48 (1H, d, *J* = 6.28 Hz, H-11a), 3.80 (3H, s, 9-OCH_3), 4.90 (1H, d, *J* = 7.41 Hz, H-1′), 3.46 (2H, overlapped, H-2′ and H-3′), 3.42 (2H, overlapped, H-4′ and H-5′), 3.88 (1H, dd, *J* = 2.11, 12.11 Hz, H-6′*α*), 3.70 (1H, dd, *J* = 5.32, 12.12 Hz, H-6′*β*); ^{13}C-NMR (125 MHz, CD_3OD): *δ* 133.3 (C-1), 111.6 (C-2), 160.2 (C-3), 105.7 (C-4), 158.0 (C-4a), 67.5 (C-6), 41.4 (C-6a), 122.6 (C-6b), 115.6 (C-7), 105.9 (C-8), 150.4 (C-9), 132.4 (C-10), 148.2 (C-10a), 80.0 (C-11a), 115.7 (C-11b), 57.0 (9-OCH_3), 102.0 (C-1′), 74.8 (C-2′), 77.9 (C-3′), 71.3 (C-4′), 78.1 (C-5′), 62.4 (C-6′).

9-*O*-Methylnissolin 3-*O*-glucoside (23) – White amorphous powder; $[\alpha]_D^{25}$ –133.55 (*c* 0.02, MeOH); ^{1}H-NMR (500 MHz, DMSO-d_6): *δ* 7.42 (1H, d, *J* = 8.63 Hz, H-1), 6.73 (1H, dd, *J* = 2.43, 8.53 Hz, H-2), 6.56 (1H, d, *J* = 2.41 Hz, H-4), 4.28 (1H, dd, *J* = 3.90, 10.20 Hz, H-6*α*), 3.67 (1H, t, *J* = 10.20 Hz, H-6*β*), 3.68 (1H, ddd, *J* = 10.20, 6.80, 3.90 Hz, H-6a), 7.00 (1H, d, *J* = 8.24 Hz, H-7), 6.53 (1H, d, *J* = 8.26 Hz, H-8), 5.63 (1H, d, *J* = 6.79 Hz, H-11a), 3.73 (3H, s, 9-OCH_3), 3.71 (3H, s, 10-OCH_3), 4.85, (1H, d, *J* = 7.54 Hz, H-1′), 3.22 (1H, m, H-2′), 3.29 (1H, m, H-3′), 3.15 (1H, m, H-4′), 3.30 (1H, m, H-5′), 4.28 (1H, m, H-6′*α*), 3.67 (1H, m, H-6′*β*); ^{13}C-NMR (125 MHz, DMSO-d_6): *δ* 132.1 (C-1), 110.5 (C-2), 158.6 (C-3), 104.0 (C-4), 156.2 (C-4a), 65.8 (C-6), 39.2 (C-6a), 121.6 (C-6b), 118.7 (C-7), 105.1 (C-8), 152.7 (C-9), 133.4 (C-10), 151.0 (C-10a), 78.2 (C-11a), 114.1 (C-11b), 56.1 (9-OCH_3), 59.9 (10-OCH_3), 100.3 (C-1′), 73.2 (C-2′), 76.6 (C-3′), 69.7 (C-4′), 77.1 (C-5′), 60.7 (C-6′).

(-)-Methylinissolin 3-*O*-*β*-D-{6″-[(*E*)-but-2-enoyl]}-glucoside (24) – Pale yellow, amorphous powder; $[\alpha]_D^{25}$ –68.47 (*c* 0.06, MeOH); ^{1}H-NMR (500 MHz, CD_3OD): *δ* 7.46 (1H, d, *J* = 8.61 Hz, H-1), 6.80 (1H, dd, *J* = 2.44, 8.54 Hz, H-2), 6.67 (1H, d, *J* = 2.42 Hz, H-4), 4.30 (1H, dd, *J* = 3.99, 10.06 Hz, H-6*α*), 3.63 (1H, t, *J* = 10.06 Hz, H-6*β*), 3.68 (1H, ddd, *J* = 10.06, 6.50, 3.99 Hz, H-6a), 6.99 (1H, d, *J* = 8.18 Hz, H-7), 6.56 (1H, d, *J* = 8.22 Hz, H-8), 5.59 (1H, d, *J* = 6.43 Hz, H-11a), 3.83 (3H, s, 9-OCH_3), 3.85 (3H, s, 10-OCH_3), 4.89 (1H, m, H-1′), 3.49 (2H, overlapped, H-2′ and H-3′), 3.39 (1H, m, H-4′), 3.71 (1H, m, H-5′), 4.52 (1H, dd, *J* = 2.14, 11.89 Hz, H-6′*α*), 4.25 (1H, dd, *J* = 7.29, 11.91 Hz, H-6′*β*), 5.92 (1H, dd, *J* = 1.74, 15.56 Hz, H-2″), 7.04 (1H, dd, *J* = 6.90, 15.55 Hz, H-3″), 1.89 (3H, dd, *J* = 1.70, 6.90 Hz, H-4″); ^{13}C-NMR (125 MHz, CD_3OD): *δ* 133.1 (C-1), 112.0 (C-2), 160.2 (C-3), 105.8 (C-4), 157.9 (C-4a), 67.6 (C-6), 41.2 (C-6a), 123.3 (C-6b), 119.9 (C-7), 106.4 (C-8), 152.6 (C-9), 135.2 (C-10), 154.4 (C-10a), 80.3 (C-11a) 115.8 (C-11b), 56.9 (9-OCH_3), 60.9 (10-OCH_3), 102.1 (C-1′), 74.8 (C-2′), 77.9 (C-3′), 71.8 (C-4′), 75.5 (C-5′), 64.7 (C-6′), 167.9 (C-1″), 123.2 (C-2″), 146.8 (C-3″), 18.2 (C-4″).

PTP1B inhibition assay – The inhibitory activity of PTP1B was evaluated via an *in vitro* assay conducted on a 96-well plate. Samples were prepared at varying concent-

rations (1–100 μM) by diluting them in a reaction buffer containing 50 mM citrate buffer (pH 6.0), 0.1 M NaCl, 1 mM EDTA (Sigma-Aldrich), and 1 mM dithiothreitol (DTT; Bio-Rad Laboratories, CA, USA). Next, 10 μL of the test samples were added to each well, followed by 30–40 μL of reaction buffer and 10 μL of PTP1B enzyme (human, recombinant; NKMAX, Korea, 5 μg/mL). The mixture was incubated at 37°C for 10 minutes before adding 50 μL of 2.0 mM *p*-NPP (Sigma-Aldrich) substrate. Then, the reaction was mixed gently and incubated again at 37°C for 20 minutes.

The reaction was stopped by adding 10 μL of 10 M NaOH, creating an alkaline environment, resulting in the formation of the yellow *p*-nitrophenolate anion. This anion absorbs at 405 nm, allowing for the determination of PTP1B inhibitory activity. Ursolic acid was included as a positive control in this experiment. The inhibition percentage was calculated using the following formula:

$$\% \text{ Inhibition} = [(\Delta \textit{ control} - \Delta \textit{ inhibition}) / \Delta \text{ control}] \times 100\%$$

Enzyme kinetic analysis – According to the PTP1B inhibition data, compounds **1**, **3**, and **19** emerged as the most potent inhibitors. Building on previous studies of compounds **1** and **3**,[22,23] this investigation aimed to explore the inhibition mechanism of compound **19**. The experimental procedure followed a similar approach to the previously described PTP1B inhibition assay, with several adjustments. The test sample was prepared at various concentrations (0, 5, 7, 10, and 20 μM) and tested against different substrate concentrations (0.5, 1.0, and 2.0 mM), resulting in distinct enzymatic reactions. The Lineweaver-Burk plot was used to analyze the data, and the inhibition mode was determined based on the intersection of the trendlines. If the lines intersected on the *x*-axis or *y*-axis, it indicated a non-competitive or competitive inhibition mode, respectively. Conversely, if the trendlines intersected in the *x*-*y* region, a mixed inhibition mode was identified. Additionally, the Dixon plot was used to calculate the inhibition constants (K_i values), which represent the binding affinity between the enzyme and the inhibitor. The figures were analyzed using Microsoft Excel 365 and visualized by Sigma plot software 15.0.

Molecular docking – Molecular docking simulations were conducted using AutoDock 4.2 software, according to our previously published protocol with a slight modification.[24] Briefly, both 2D and 3D conformers of vesticarpan (**19**) were constructed by ChemBioOffice 16.0. The PTP1B structure and its reference catalytic inhibitor [3-({5-[(*N*-acetyl-3-{4-[(carboxycarbonyl) (2-carboxyphenyl)amino]-1-naphthyl}-L-alanyl)amino]pentyl}oxy)-2-naphthoic acid (compound C; PDB ID: 1NNY)] were obtained from the Protein Data Bank website (https://www.rcsb.org). A Lamarckian genetic algorithm method implemented in AutoDock 4.2 was employed. For docking calculations, Gasteiger charges were added by default, the rotatable bonds were set by the AutoDock Tools, and all torsions were allowed to rotate. The docking protocol for rigid and flexible ligand docking consisted of 15 independent Genetic Algorithms, while other parameters were used as defaults for the AutoDock Tools. The interactions of protein-ligand complexes were analyzed and visualized using PyMOL and Discovery Studio Visualizer 16.1 (Accelrys, Inc. San Diego, CA, USA).

Statistical analysis – The data were presented as means ± standard error of the mean (SEM) based on three replicates. Duncan's test and ANOVA were applied to assess statistical significance at $p < 0.05$.

Results and Discussion

The structures of all isolated compounds were determined using 1D and 2D NMR spectroscopy. After the spectroscopic analysis, the obtained structures were compared with the relevant data from published studies. Therefore, the structures of 24 flavonoids were identified as formonentin (**1**),[25] calycosin (**2**),[26] pratensein (**3**),[27] afromorsin (**4**),[28] odoratin (**5**),[29] ononin (**6**),[30] 6″-*O*-Acetylononin (**7**),[31] calycosin 7-*O*-*β*-D-glucoside (**8**),[32] calycosin 7-*O*-*β*-D-glucoside-6″-*O*-acetate (**9**),[33] calycosin 7-*O*-*β*-D-{6″-[(*E*)-but-2-enoyl]}-glucoside (**10**),[34] isomucronulatol (**11**),[35] isomucronulatol 7-*O*-*β*-glucoside (**12**),[36] 2′-hydroxy-3′,4′-dimethoxyisoflavan 7-*O*-*β*-D-glucoside 6″-*O*-acetate (**13**),[36] isomucronulatol 2′,7-diglucoside (**14**),[37] pendulone (**15**),[38] 4,7,2′-Trihydroxy-4′-methoxyisoflavanol (**16**),[39] (2*S*)-liquiritigenin (**17**),[40] isoliquiritigenin (**18**),[41] vesticarpan (**19**),[41] methylnissolin (**20**),[41] (6a*R*,11a*R*)-3,8-dihydroxy-9,10-dimethoxypterocarpan (**21**),[41] licoagroside D (**22**),[42] 9-*O*-methylnissolin 3-*O*-glucoside (**23**),[33] (-)-methylinissolin 3-*O*-*β*-D-{6″-[(*E*)-but-2-enoyl]}-glucoside (**24**),[33] (Fig. 1).

All isolated compounds were evaluated for their PTP1B inhibitory activity. As illustrated in Table 1, compared to ursolic acid (IC_{50} 8.9 ± 1.70 μM), formonentin (**1**), pratensein (**3**), and vesticarpan (**19**) standed out as the promissing PTP1B inhibitors with IC_{50} values of 10.9 ± 1.09 μM, 10.0 ± 1.71 μM, and 10.3 ± 1.31 μM, respectively.

According to the structure-activity relationship among isoflavones (Fig. 2), compounds **1** and **3** emerged as the most effective inhibitors, suggesting that the hydroxy

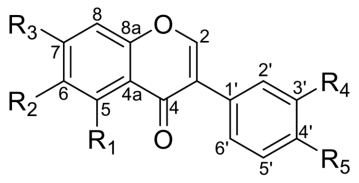

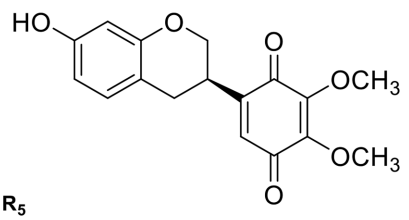

	R_1	R_2	R_3	R_4	R_5
1	H	H	OH	H	OCH_3
2	H	H	OH	OH	OCH_3
3	OH	H	OH	OH	OCH_3
4	H	OCH_3	OH	H	OCH_3
5	H	OCH_3	OH	OH	OCH_3
6	H	H	*O*-*β*-Glc	H	OCH_3
7	H	H	*O*-*β*-D-glucoside 6″-*O*-acetate	H	OCH_3
8	H	H	*O*-*β*-Glc	OH	OCH_3
9	H	H	*O*-*β*-D-glucoside 6″-*O*-acetate	OH	OCH_3
10	H	H	*O*- *β*-D-[6-(*E*)-but-enoyl]-glucose	OH	OCH_3

15

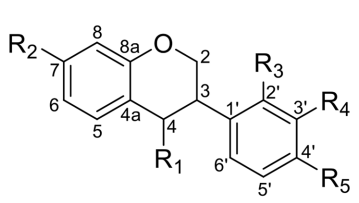

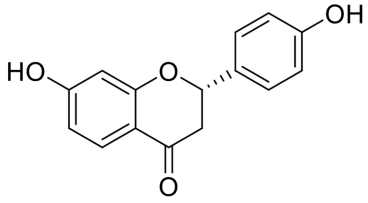

	R_1	R_2	R_3	R_4	R_5
11	H	OH	OH	OCH_3	OCH_3
12	H	*O*-*β*-Glc	OH	OCH_3	OCH_3
13	H	*O*-*β*-D-glucoside 6″-*O*-acetate	OH	OCH_3	OCH_3
14	H	*O*-*β*-Glc	*O*-*β*-Glc	OCH_3	OCH_3
16	OH	OH	OH	H	OCH_3

17

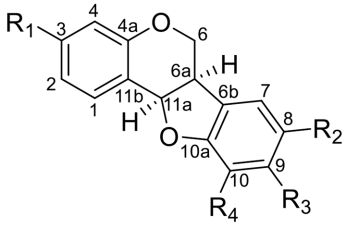

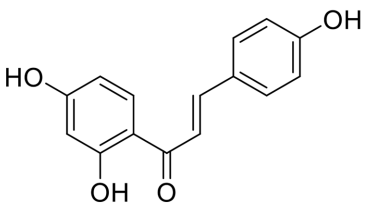

	R_1	R_2	R_3	R_4
19	OH	H	OCH_3	OH
20	OH	H	OCH_3	OCH_3
21	OH	OH	OCH_3	OCH_3
22	*O*-*β*-Glc	H	OCH_3	OH
23	*O*-*β*-Glc	H	OCH_3	OCH_3
24	*O*-*β*-D-[6-(*E*)-but-enoyl]-glucose	H	OCH_3	OCH_3

18

Fig. 1. Chemical structure of flavonoids (**1**–**24**) isolated from the roots of *A. membranaceus*.

groups at C-5 and C-7, along with the methoxy group at C-4′, play a crucial role in their activity. In contrast, compounds **2**, **4**, and **6** showed no inhibitory effects (IC_{50} > 100 μM), indicating that the presence of a hydroxy group at C-3′, a methoxy group at C-6, or a glucose moiety at C-7 hindered inhibition. Additionally, compounds **7** and **9** demonstrated moderate inhibition, highlighting that the acetyl group at C-6″ significantly influences their inhibitory activity.

Furthermore, as showed in Fig. 3, among the pterocarpans, compound **19** emerged as the most potent inhibitor (IC_{50} 10.3 ± 1.31 μM). In contrast, compounds **20**, **21**, **22**, and

Table 1. PTP1B inhibitory activity of isolated compounds (**1**–**24**)

Compound	PTP1B inhibition		
	IC_{50} (μM)[a]	Inhibition type[b]	K_i (μM)[c]
1	10.9 ± 1.09	-	-
2	> 100	-	-
3	10.0 ± 1.71	-	-
4	> 100	-	-
5	46.0 ± 2.46	-	-
6	> 100	-	-
7	35.6 ± 1.61	-	-
8	> 100	-	-
9	38.0 ± 2.16	-	-
10–14	> 100	-	-
15	15.3 ± 0.27	-	-
16	40.2 ± 2.32	-	-
17	42.5 ± 1.25	-	-
18	19.8 ± 3.10	-	-
19	10.3 ± 1.31	Competitive	7.6 ± 1.17
20	> 100	-	-
21	61.7 ± 1.37	-	-
22–23	> 100	-	-
24	33.8 ± 5.61	-	-
Ursolic acid[d]	8.9 ± 1.70	-	-

[a] The values (μM) indicate 50% inhibitory activity and are presented as the mean ± SEM from three independent experiments
[b] Determined by Lineweaver-Burk plots
[c] Determined by Dixons plots
[d] Positive control
(-) No test

23 exhibit minimal to no effect on PTP1B. The potent inhibitory activity of **19** is attributed to its hydroxy groups at C-3 and C-10 and a methoxy group at C-9. The results also revealed that the methoxy group at C-10 (in **20**, **21**, and **23**) and the glucose moiety at C-3 (in **22**) diminished PTP1B inhibition. However, despite similar structural features, compound **24** exhibited moderate inhibitory activity (IC_{50} 33.8 ± 5.61 μM), suggesting that the (*E*)-but-2-enoyl group at C-6″ enhances its ability to inhibit PTP1B.

Building on the observed inhibitory effects and the existing data on the PTP1B inhibitory activity of compounds **1** and **3**,[22,23] this study conducted an enzyme kinetic assay to primarily elucidate the inhibition mode and inhibition constant (K_i) of compound **19**. The type of inhibition was identified by analyzing the intersection points of trendlines, which illustrated the variations in inhibitory effects at different test sample concentrations across varying substrate levels. In particular, convergence at the *x*-axis indicated non-competitive inhibition, while intersection at the *y*-axis signified competitive mode. Alternatively, convergence within the *x*-*y* plane was indicative of mixed-type inhibition.[43] As shown in Fig. 4A, the Lineweaver-Burk plot revealed that the trendlines converged at the *y*-axis, indicating that compound **19** inhibits PTP1B through a competitive mechanism. This finding suggested that compound **19** interacted with PTP1B at the active site, competing with the substrate at the same binding site, causing changes in the conformational dynamics of the enzymes, resulting in the diminishment of the enzyme's function. Meanwhile, the Dixon plot (Fig. 4B) revealed the K_i value to be 7.6 ± 1.17 μM, represented by the intersection point of the lines

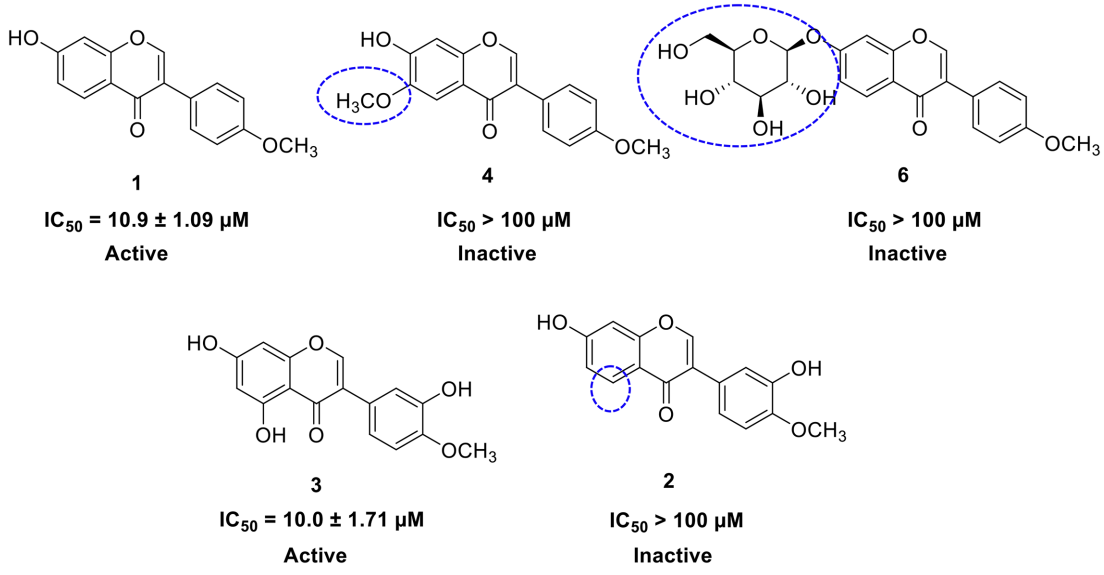

Fig. 2. Structure-activity relationship analysis of the isoflavones.

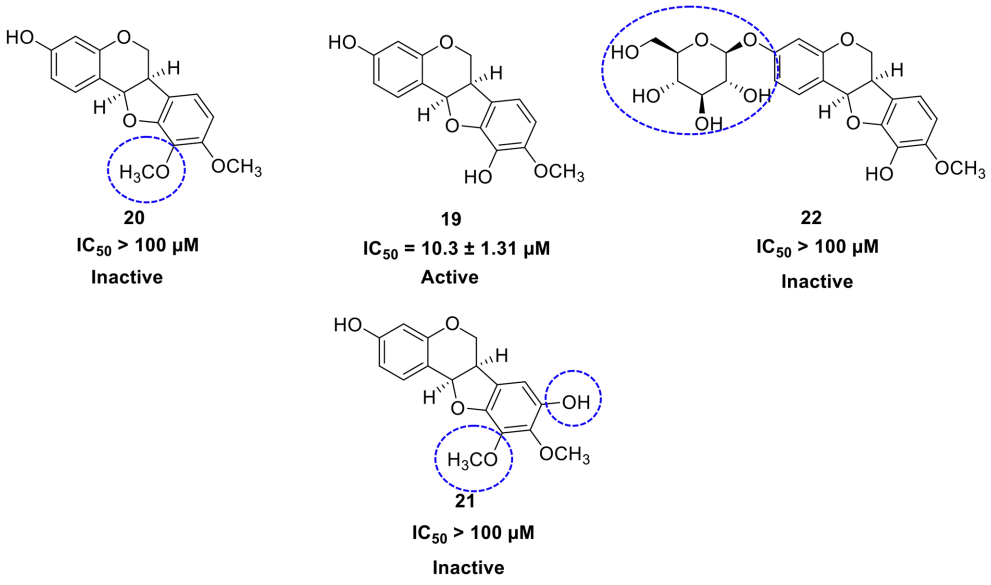

Fig. 3. Structure-activity relationship analysis of the pterocarpans.

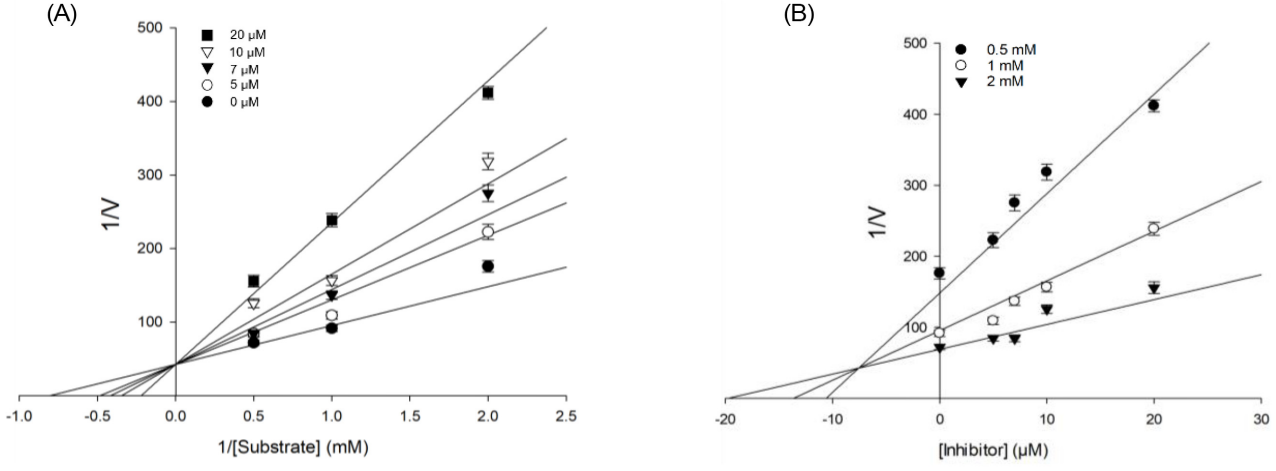

Fig. 4. Lineweaver-Burk (A) and Dixon plots (B) for PTP1B inhibitory activity of compound **19**.

on the *x*-axis. This K_i value corresponds to the dissociation constant of the inhibitor-enzyme complex, providing a measure of binding strength. A smaller K_i indicates a higher binding affinity, signifying that lower inhibitor concentrations are sufficient to suppress enzyme activity effectively.

Based on the enzyme kinetic analysis, molecular docking simulations were conducted to evaluate the binding interactions of compound **19** with PTP1B. The kinetic data demonstrated that compound **19** acts as a competitive inhibitor against PTP1B, suggesting that its docking site is localized within the protein's catalytic region (Fig. 5A).

As shown in Table 2, compound **19** demonstrated significant interactions with PTP1B, exhibiting a binding energy of −6.69 kcal/mol, surpassing compound C, a catalytic inhibitor, with a binding energy of −8.05 kcal/mol. These interactions were primarily mediated through van der Waals forces and hydrogen bonds. Specifically, van der Waals interactions were observed with residues Gly218, Gln262, Thr263, Gly183, Lys116, and Trp179. Hydrogen bonds were formed between the hydroxyl group at C-3 and residues Cys215, Ser216, and Ala217, as well as between the hydroxyl group at C-10 and Asp181. Additionally, the oxygen atoms in the cyclohexane and cyclopentane rings formed hydrogen bonds with Gln266 and Arg221, respectively. Furthermore, the interaction was

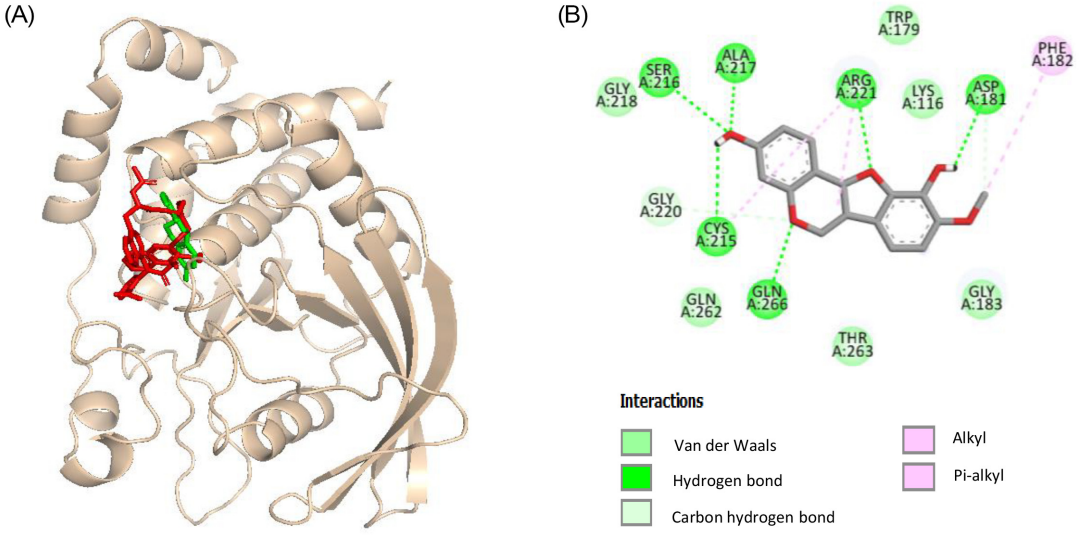

Fig. 5. Molecular docking related PTP1B inhibition by compound C (red stick), **19** (green stick) (A), and 2D diagram of PTP1B inhibition by compound **19** (B).

Table 2. Binding energy and interactions of compound (**19**) and the reference inhibitor (compound C) with PTP1B

Compound	Binding energy (kcal/mol)	Van der waals	Hydrogen bond	Other interactions		
				Alkyl	π-alkyl	Others
19	−6.69	Gly218, Gln262, Thr263, Gly183, Lys116, Trp179	Ser216, Ala217, Cys215, Gln266, Arg221, Asp181	Phe182, Arg221	Arg221, Cys215	-
C (catalytic inhibitor)	−8.05	Gln262, Gln266, Thr263, Trp197, Tyr20, Arg24, Tyr46, Glu115	Gly220, Il2219, Cys215, Ala217, Ser216, Gly218, Lys116	Ile219, Ala217	Arg221, Lys120	-

strengthened by alkyl bonds with Phe182 and Arg221 and π-alkyl bonds with Arg221 and Cys215, further reinforcing the ligand-protein binding (Fig. 5B).

In summary, this study provides the first evidence of the therapeutic potential of flavonoids from the roots of *A. membranaceus* in diabetes treatment via PTP1B inhibition. Notably, formononetin (**1**), pratensein (**3**), and vesticarpan (**19**) exhibited significant inhibitory effects against PTP1B, underscoring the potential of the flavonoid fraction in diabetic therapy. In particular, identifying vesticarpan (**19**) as a novel PTP1B inhibitor serves as the foundation for further investigations to support the development of new therapeutic agents for diabetes treatment.

Acknowledgments

This research was supported by the National Research Foundation of Korea (NRF) funded by the Korea government (MSIT) (No. NRF-2020R1A5A2017323). The authors would like to thank Korea Basic Science Institute (KBSI) Daegu Center for the mass spectra measurement service.

Conflicts of Interest

The authors declare that they have no conflicts of interest.

References

(1) Arroyave, F.; Montaño, D.; Lizcano, F. *Int. J. Mol. Sci.* **2020**, *21*, 8685.
(2) Krause, M.; De Vito, G. *Nutrients* **2023**, *15*, 4279.
(3) Zakir, M.; Ahuja, N.; Surksha, M. A.; Sachdev, R.; Kalariya, Y.; Nasir, M.; Kashif, M.; Shahzeen, F.; Tayyab, A.; Khan, M. S. M.; Junejo, M.; Kumar, F. M.; Varrassi, G.; Kumar, S.; Khatri, M.; Mohamad, T.; *Cureus* **2023**, *15*, e45835.
(4) Rani, P. K.; Raman, R.; Gella, L.; Kulothungan, V.; Sharma, T. *Middle East Afr. J. Ophthalmol.* **2012**, *19*, 129–134.
(5) Bansal, D.; Gudala, K.; Muthyala, H.; Esam, H. P.; Nayakallu, R.; Bhansali, A. *J. Diabetes Investig.* **2014**, *5*, 714–721.
(6) Pathak, V.; Pathak, N. M.; O'Neill, C. L.; Guduric-Fuchs, J.; Medina, R. J. *Clin. Med. Insights Endocrinol. Diabetes* **2019**, *12*, 1179551419844521.
(7) Johnson, T. O.; Ermolieff, J.; Jirousek, M. R. *Nat. Rev. Drug Discov.* **2002**, *1*, 696–709.
(8) Cho, H. *Vitam. Horm.* **2013**, *91*, 405–424.
(9) Thiebaut, P. A.; Besnier, M.; Gomez, E.; Richard, V. *J. Mol. Cell. Cardiol.* **2016**, *101*, 50–57.
(10) Heinonen, K. M.; Tremblay, M. L. *Cell Cycle* **2006**, *5*, 1053–1056.
(11) Liu, Z.; Gao, H.; Zhao, Z.; Huang, M.; Wang, S.; Zhan, J. *Biomed.*

Pharmacother. **2023**, *157*, 113990.
(12) Ullah, A.; Munir, S.; Badshah, S. L.; Khan, N.; Ghani, L.; Poulson, B. G.; Emwas, A.-H.; Jaremko, M. *Molecules* **2020**, *25*, 5243.
(13) AL-Ishaq, R. K.; Abotaleb, M.; Kubatka, P.; Kajo, K.; Büsselberg, D. *Biomolecules* **2019**, *9*, 430.
(14) Yang, L.-P.; Shen, J.-G.; Xu, W.-C.; Li, J.; Jiang, J.-Q. *Chem. Biodivers.* **2013**, *10*, 1004–1054.
(15) Abdel-Latif, H. M. R.; Ahmed, H. A.; Shukry, M.; Chaklader, M. R.; Saleh, R. M.; Khallaf, M. A. *Fishes* **2022**, *7*, 319.
(16) Wang, H.-P.; Lin, Z.-Z.; Zhao, C.; Yin, Q.; Jia, J. *J. Asian Nat. Prod. Res.* **2024**, *26*, 1348–1357.
(17) Wu, Y.; Ou-Yang, J.-P.; Wu, K.; Wang, Y.; Zhou, Y.-F.; Wen, C.-Y. *Acta Pharmacol. Sin.* **2005**, *26*, 345–352.
(18) Wang, N.; Zhang, D.; Mao, X.; Zou, F.; Jin, H.; Ouyang, J. *Mol. Cell. Endocrinol.* **2009**, *307*, 89–98.
(19) Zhou, X.; Wang, L. L.; Tang, W. J.; Tang, B. *J. Ethnopharmacol.* **2021**, *268*, 113556.
(20) Wang, Z.; Li, X.-L.; Hong, K.-F.; Zhao, T.-T.; Dong, R.-X.; Wang, W.-M.; Li, Y.-T.; Zhang, G.-L.; Lin,-J.; Gui, D.-K.; Xu, Y.-H. *Evid. Based Complement. Alternat. Med.* **2021**, *2021*, 6675567.
(21) Lee, D.; Lee, D. H.; Choi, S.; Lee, J. S.; Jang, D. S.; Kang, K. S. *Biomolecules* **2019**, *9*, 618.
(22) Wang, J.; Wang, L.; Han, L.; Han, Y.; Gu, J.; Chen, Z. *Int. Immunopharmacol.* **2024**, *140*, 112802.
(23) Zhao, B. T.; Le, D. D.; Nguyen, P. H.; Ali, M. Y.; Choi, J.-S.; Min, B. S.; Shin, H. M.; Rhee, H. I.; Woo, M. H. *Chem. Biol. Interact.* **2016**, *253*, 27–37.
(24) Ha, M. T.; Lee, T. H.; Kim, C. S.; Prajapati, R.; Kim, J. A.; Choi, J. S.; Min, B. S. *Phytochemistry* **2022**, *197*, 113100.
(25) Li, S.-R.; Chen, P.-Y.; Chen, L.-Y.; Lo, Y.-F.; Tsai, I.-L.; Wang, E.-C. *Tetrahedron Lett.* **2009**, *50*, 2121–2123.
(26) Salem, M. M.; Werbovetz, K. A. *J. Nat. Prod.* **2006**, *69*, 43–49.
(27) Lin, Y.-L.; Tsai, W.-J.; Chen, I.-S.; Kuo, Y. H. *J. Chin. Chem. Soc.* **1998**, *45*, 213–217.
(28) Goto, H.; Terao, Y.; Akai, S. *Chem. Pharm. Bull.* **2009**, *57*, 346–360.
(29) Velozo, L. S. M.; da Silva, B. P.; Bernardo, R. R.; Parente, J. P. *Phytochemistry* **1999**, *52*, 1473–1477.
(30) Han, T.; Li, H.; Zhang, Q.; Zheng, H.; Qin, L. *Chem. Nat. Compd.* **2006**, *42*, 567–570.
(31) Barrero, A. F.; Sanchez, J. F.; Barrón, A.; Corrales, F.; Rodriguez, I. *Phytochemistry* **1989**, *28*, 161–164.
(32) Du, X.; Bai, Y.; Liang, H.; Wang, Z.; Zhao, Y.; Zhang, Q.; Huang, L. *Magn. Reson. Chem.* **2006**, *44*, 708–712.
(33) Zhang, L.-J.; Liu, H.-K.; Hsiao, P.-C.; Kuo, L.-M. Y.; Lee, I.-J.; Wu, T.-S.; Chiou, W.-F.; Kuo, Y.-H. *J. Agric. Food Chem.* **2011**, *59*, 1131–1137.
(34) Pei, Y.; Li, R.; Fu, H.; Wang, J.; Zhou, Y. *Fitoterapia* **2007**, *78*, 602–604.
(35) Guo, K.; He, X.; Zhang, Y.; Li, X.; Yan, Z.; Pan, L.; Qin, B. *Fitoterapia* **2016**, *114*, 34–39.
(36) Ma, X.; Tu, P.; Chen, Y.; Zhang, T.; Wei, Y.; Ito, Y. *J. Chromatogr. A.* **2004**, *1023*, 311–315.
(37) Subarnas, A.; Oshima, Y.; Hikino, H. *Phytochemistry* **1991**, *30*, 2777–2780.
(38) Radwan, M. M. *Nat. Prod. Commun.* **2008**, *3*, 1491–1494.
(39) Bojase, G.; Wanjala, C. C. W.; Majinda, R. R. T. *Bull. Chem. Soc. Ethiop.* **2001**, *15*, 131–136.
(40) Ogata, T.; Yahara, S.; Hisatsune, R.; Konishi, R.; Nohara, T. *Chem. Pharm. Bull.* **1990**, *38*, 2750-2755.
(41) Piccinelli, A. L.; Campo Fernandez, M.; Cuesta-Rubio, O.; Márquez Hernández, I.; De Simone, F.; Rastrelli, L. *J. Agric. Food. Chem.* **2005**, *53*, 9010–9016.
(42) Li, W.; Koike, K.; Asada, Y.; Hirotani, M.; Rui, H.; Yoshikawa, T.; Nikaido, T. *Phytochemistry* **2002**, *60*, 351–355.
(43) Phong, N. V.; Oanh, V. T.; Yang, S. Y.; Choi, J. S.; Min, B. S.; Kim, J. A. *Int. J. Biol. Macromol.* **2021**, *188*, 719–728.

Received February 18, 2025
Revised March 22, 2025
Accepted March 25, 2025